Inorg. Chem. **1982**, *21*, 2483–2487

Contribution from the Department of Applied Chemistry,
Faculty of Engineering, Osaka University, Suita, Osaka 565, Japan

Kinetic and Mechanistic Studies on the Reaction of (Trithioperoxybenzoato)(dithiobenzoato)oxomolybdenum(IV), $MoO(S_3CC_6H_5)(S_2CC_6H_5)$, with Tertiary Phosphines

KOJI TANAKA, KAZUSHI KONDO, and TOSHIO TANAKA*

Received December 22, 1981

Kinetics of the reaction of (trithioperoxybenzoato)(dithiobenzoato)oxomolybdenum(IV), $MoO(S_3CC_6H_5)(S_2CC_6H_5)$, with tertiary phosphine, R_3P (R = *n*-Bu, C_6H_5), was investigated in 1,2-dichloroethane by the use of a stopped-flow spectrophotometer under pseudo-first-order conditions with excess R_3P. The result has revealed that $MoO(S_3CC_6H_5)(S_2CC_6H_5)$ undergoes sulfur abstraction by *n*-Bu_3P to give $MoO(S_2CC_6H_5)_2$, which further reacts with excess Bu_3P, affording an intermediate involving the charge-transfer interaction between the $S_2CC_6H_5$ moiety and *n*-Bu_3P. The subsequent rearrangement of the intermediate proceeds in a zero-order kinetics with respect to the phosphine concentration, yielding *cis*-$MoO(S_2CC_6H_5)_2$(*n*-Bu_3P). The intermediate is stable below −40 °C, and the structure is proposed on the basis of ^{13}C and ^1H NMR spectra. A similar sulfur abstraction from the $S_3CC_6H_5$ moiety by Ph_3P occurs. The subsequent reaction of $MoO(S_2CC_6H_5)_2$ with excess Ph_3P, however, gives no charge-transfer complex between the $S_2CC_6H_5$ moiety and Ph_3P but an equilibrium mixture of *trans*- and *cis*-$MoO(S_2CC_6H_5)_2(Ph_3P)$ and the dissociated species in solution. The difference in mechanisms between the reactions of Ph_3P and *n*-Bu_3P toward $MoO(S_2CC_6H_5)_2$ is interpreted in terms of the donor properties of these phosphines.

Introduction

Oxomolybdenum complexes containing dithio chelate ligands have been of interest as possible model compounds for molybdo enzymes.[1,2] Of those, bis(dithiocarbamato)dioxomolybdenum(VI) is well-known to catalyze the air oxidation of tertiary phosphine, which involves oxo abstraction reactions from the dioxomolybdenum complex by the phosphine.[3,4] On the other hand, sulfur abstraction is known to occur in the reaction of (trithioperoxycumato)(dithiocumato)nickel(II), $Ni(S_3CC_6H_4C_3H_7)(S_2CC_6H_4C_3H_7)$, with Ph_3P to give $Ni(S_2CC_6H_4C_3H_7)_2$ and Ph_3PS.[5,6] There is, however, no report on sulfur abstraction from molybdenum complexes so far.

One of the authors has recently reported the preparation and the X-ray structure analysis of (trithioperoxybenzoato)(dithiobenzoato)oxomolybdenum(IV), $MoO(S_3CC_6H_5)(S_2CC_6H_5)$.[7,8] The sulfur atom adjacent to carbon in the trithioperoxybenzoato ligand is expected to be labile by analogy with the trithioperoxycumato ligand coordinated to nickel.[5,6] This paper reports the kinetics and mechanism of the reaction of $MoO(S_3CC_6H_5)(S_2CC_6H_5)$ with excess R_3P (R = *n*-Bu, C_6H_5), which consists of the sulfur abstraction from the trithioperoxybenzoato ligand and the subsequent addition reaction of R_3P toward $MoO(S_2CC_6H_5)_2$.

Experimental Section

Materials. 1,2-Dichloroethane used as a solvent for kinetic and spectroscopic measurements was purified in the usual manner.[9] Commercially available tributylphosphine was purified by distillation; bp 88 °C (5 mmHg). (Trithioperoxybenzoato)(dithiobenzoato)oxomolybdenum(IV), MoO(ttb)(dtb) (ttb = $S_3CC_6H_5$, dtb = $S_2CC_6H_5$), bis(dithiobenzoato)oxomolybdenum(IV), $MoO(dtb)_2$, and the tertiary phosphine adducts, $MoO(dtb)_2(R_3P)$ (R = *n*-Bu, Ph), were prepared described elsewhere.[8]

(Trithioperoxy-*p*-toluato)(dithio-*p*-toluato)oxomolybdenum(IV), MoO(ttt)(dtt) (ttt = $S_3CC_6H_4Me$-*p*; dtt = $S_2CC_6H_4Me$-*p*), was obtained as follows: to an aqueous solution (200 cm^3) of $Na_2S_2O_4$ (16.0 g, 80 mmol) was added an aqueous solution (300 cm^3) containing $Na_2MoO_42H_2O$ (3.37 g, 14.9 mmol) and $(Et_2NH_2^+)(p\text{-}MeC_6H_4CS_2^-)$ (3.83 g, 14.9 mmol). After 18 h of stirring at room temperature, the solution was mixed with hydrochloric acid (5.0 mol dm^{-3}, 100 cm^3). The resulting solution was stirred for an additional 1 h to give a precipitate, which was collected by filtration and washed several times with water. The product was recrystallized from a mixture of benzene–petroleum ether to yield red needles in a 15% yield; mp 173–174 °C. Anal. Calcd for $C_{16}H_{14}OS_5Mo$: C, 40.16; H, 2.95. Found: C, 40.12; H, 3.05.

Reaction of MoO(ttt)(dtt) with R_3P (R = *n*-Bu, Ph). An equimolar reaction of MoO(ttt)(dtt) (1.70 g, 3.56 mmol) with R_3P (0.72 g for R = *n*-Bu, 0.93 g for R = Ph) in CH_2Cl_2 (30 cm^3) afforded dark brown crystals of $MoO(dtt)_2$ in a 90% yield by the procedure quite similar to that of MoO(ttb)(dtb) with Ph_3P, as described elsewhere;[8] 190 °C dec. Anal. Calcd for $C_{16}H_{14}OS_4Mo$: C, 43.04; H, 3.14. Found: C, 43.12; H, 3.41. On the other hand, the reaction of MoO(ttt)(dtt) (0.16 g, 0.36 mmol) with two equivalent amounts of *n*-Bu_3P (0.15 g) in benzene (15 cm^3) gave yellow plates of $MoO(dtt)_2$(*n*-Bu_3P) in a 80% yield; 180 °C dec. Anal. Calcd for $C_{28}H_{42}OPS_4Mo$: C, 51.85; H, 6.33. Found: C, 51.46; H, 6.54. This reaction also is analogous to that between MoO(ttb)(dtb) and excess *n*-Bu_3P, which was reported previously.[8]

Spectra. Electronic and infrared spectra were recorded on a Union SM-401 and a Hitachi 215 spectrophotometer, respectively. Proton and ^{13}C NMR spectra were measured at 100 MHz with a JEOL PS-100 spectrometer and at 15.3 MHz with use of the pulse Fourier technique with a JEOL EX-60 spectrometer, respectively, both with Me_4Si as the internal standard.

Kinetic Measurements. Kinetic experiments were carried out under pseudo-first-order conditions with at least a 10-fold excess amount of tertiary phosphine. The rate of reaction was followed by monitoring the absorbance at a fixed wavelength in the electronic spectra of the reaction mixture with a Union RA-1100 stopped-flow spectrophotometer equipped with a 2- or 10-mm quartz cell. The measurements were usually made over a period of 3 half-lives of the reaction. Pseudo-first-order rate constants, k_{obsd}, were obtained from the semilogarithmic plots of $\ln(A_t - A_\infty)$ against time, where A_t and A_∞ are absorbances at a given wavelength at time t and at the end of the reaction, respectively. Rapid-scanning spectra were measured with a Union RA-1100 stopped-flow reaction analyzer in order to determine the wavelength by which the reaction can best be followed.

Results and Discussion

Stoichiometry of the Reactions and the Reaction Products in Solution. An equimolar reaction of MoO(ttb)(dtb) with *n*-Bu_3P in CH_2Cl_2 gave *n*-Bu_3PS and $MoO(dtb)_2$ almost quantitatively. The latter compound further reacted with

---

(1) Stiefel, E. I. *Prog. Inorg. Chem.* **1977**, *22*, 1.

(2) Wentworth, R. A. D. *Coord. Chem. Rev.* **1976**, *18*, 1.

(3) Chen, G. J. J.; McDonald, J. W.; Newton, W. E. *Inorg. Chem.* **1976**, *15*, 2612.

(4) Nakamura, A.; Ueyama, N. "Molybdenum Chemistry of Biological Significance"; Newton, W. E., Otsuka, Sei, Eds.; Plenum Press: New York, 1979; p 369.

(5) Fackler, J. P., Jr.; Fetchin, J. A.; Fries, David C. *J. Am. Chem. Soc.* **1972**, *94*, 7323.

(6) Coucouvanis, D.; Fackler, J. P., Jr. *J. Am. Chem. Soc.* **1967**, *89*, 1346.

(7) Tatsumisago, M.; Matsubayashi, G.; Tanaka, T.; Nishigaki, S.; Nakatsu, K. *Chem. Lett.* **1979**, 889.

(8) Tatsumisago, M.; Matsubayashi, G.; Tanaka, T.; Nishigaki, S.; Nakatsu, K. *J. Chem. Soc., Dalton Trans*, in press.

(9) Riddick, J. A.; Toops, E. E., Jr. "Technique of Organic Chemistry", 2nd ed.; Weissberger, A., Ed.; Interscience: New York, 1955; Vol. 7, p 416.

0020-1669/82/1321-2483$01.25/0

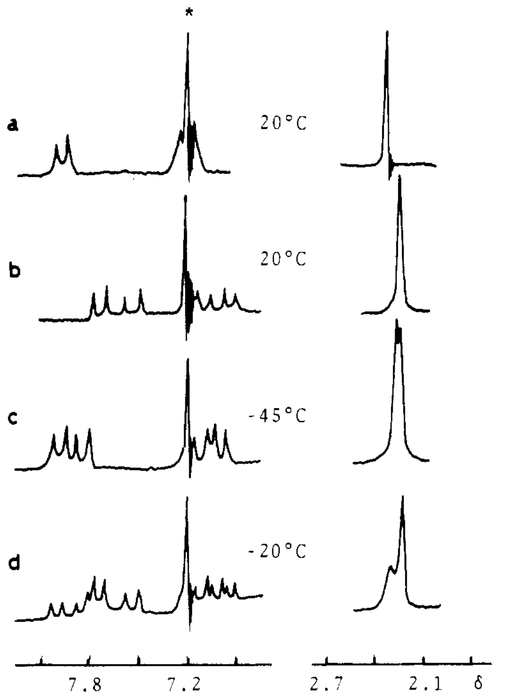

Figure 1. ^{1}H NMR spectra of $MoO(dtt)_2$ (a) and $MoO(dtt)_2(n\text{-}Bu_3P)$ (b) and an equimolar solution of $MoO(dtt)_2$ and $n\text{-}Bu_3P$ at −45 °C (c) and −20 °C (d) in $CDCl_3$; the equimolar solution was prepared at −45 °C.

$n\text{-}Bu_3P$ to afford the 1:1 adduct $MoO(dtb)_2(n\text{-}Bu_3P)$, which was obtained also by the reaction of MoO(ttb)(dtb) with excess $n\text{-}Bu_3P$.[8] The infrared spectrum of $MoO(dtb)_2(n\text{-}Bu_3P)$ showed only a ν(Mo═O) band at 945 cm^{-1} not only in the solid state but also in a CS_2 solution. This wavenumber is 25 cm^{-1} lower than that of $MoO(dtb)_2$, indicating the coordination of $n\text{-}Bu_3P$ to the Mo atom. The configurations of $MoO(dtb)_2$ and $MoO(dtb)_2$ ($n\text{-}Bu_3P$) in solution are inquired from the ^{1}H NMR spectra of the dithiotoluato analogues $MoO(dtt)_2$ and $MoO(dtt)_2(n\text{-}Bu_3P)$. The $MoO(dtt)_2$ complex exhibits a singlet signal (δ 2.41) and an AB-type quartet signal (δ 7.21, 8.05; J = 8 Hz) due to the methyl and phenyl ring protons in $CDCl_3$, respectively, as shown in Figure 1a. This is consistent with the square-pyramidal configuration (**1**) of $MoO(dtt)_2$, as is

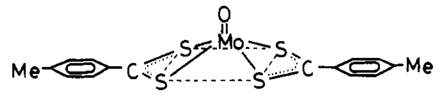

1

well-known for bis(N,N-dipropyldithiocarbamato)oxomolybdenum(IV), $MoO(S_2CN\text{-}n\text{-}Pr_2)_2$.[10] On the other hand, the ^{1}H NMR spectrum of $MoO(dtt)_2(n\text{-}Bu_3P)$ shows two quartet signals, as seen in Figure 1b. This observation clearly indicates the presence of magnetically nonequivalent tolyl groups, although the methyl proton signal occurs as a singlet. Thus, $MoO(dtt)_2(n\text{-}Bu_3P)$ is suggested to assume the cis configuration (**2**).

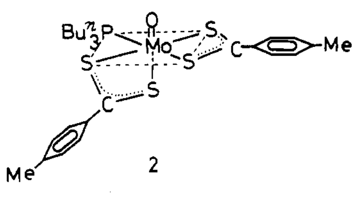

2

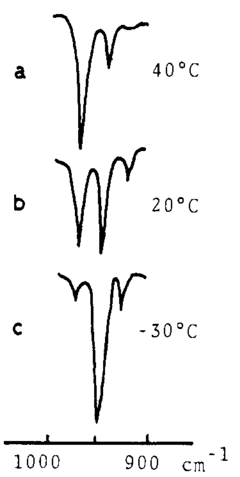

Figure 2. Mo═O stretching bands of $MoO(dtb)_2(Ph_3P)$ in CS_2 at various temperatures.

The MoO(ttb)(dtb) complex reacted also with equimolar or excess Ph_3P in CH_2Cl_2 to give $MoO(dtb)_2$ or $MoO(dtb)_2(Ph_3P)$. The infrared spectrum of $MoO(dtb)_2(Ph_3P)$ in CS_2 at 40 °C exhibits a strong ν(Mo═O) band at 970 cm^{-1} and a weak one at 948 cm^{-1} as shown in Figure 2a, although the Nujol mulls spectrum displayed only a strong ν(Mo═O) band at 952 cm^{-1}. In addition, the appearance of the solution spectra varies with temperature; when the temperature is lowered, an additional new band appears at 932 cm^{-1} and the 948-cm^{-1} band concurrently increases in intensity at the expense of the 970-cm^{-1} band (Figure 2b), which is fairly weakened at −30 °C (Figure 2c). The band at 970 cm^{-1} can be associated with $MoO(dtb)_2$ without coordination of Ph_3P because the authentic sample of $MoO(dtb)_2$ in CS_2 exhibited ν(Mo═O) at the same wavenumber. The existence of $MoO(dtb)_2$ in solution may be due to the weaker donor ability of Ph_3P than $n\text{-}Bu_3P$, whose adduct with $MoO(dtb)_2$ or $MoO(dtt)_2$ shows no appreciable dissociation in solution, as described above. On the other hand, the 948- and 932-cm^{-1} bands are assigned to the ν(Mo═O) of the $MoO(dtb)_2(Ph_3P)$ species tentatively; the former may be due to the cis isomer and the latter to the trans isomer, as described later. Thus, the adduct $MoO(dtb)_2(Ph_3P)$ formed in the reaction may exist as an equilibrium mixture of cis and trans isomers and the dissociative species in solution.

Intermediates Formed in the Reaction of MoO(ttb)(dtb) with *n*-Bu$_3$P. The electronic spectra of MoO(ttb)(dtb) and $MoO(dtb)_2$ in CH_2ClCH_2Cl show an absorption maximum at 404 nm (ε 1.0 × 10^4 M^{-1} cm^{-1}) as well as 338 nm (ε 2.5 × 10^4 M^{-1} cm^{-1}) and 370 nm (ε 3.4 × 10^4 M^{-1} cm^{-1}) as depicted in Figure 3a. Neither $n\text{-}Bu_3P$ nor the 1:1 adduct, $MoO(dtb)_2(n\text{-}Bu_3P)$, exhibited appreciable absorption in the visible region. Immediately after MoO(ttb)(dtb) is mixed with at least 2 equiv of $n\text{-}Bu_3P$ in CH_2ClCH_2Cl, the solution develops an absorption maximum at 517 nm as well as 330 nm, as shown in Figure 3b. This band almost disappeared with a half-life of 10 s, and the final spectrum obtained in 3 min after mixing (Figure 3b) was consistent with that of authentic $MoO(dtb)_2(n\text{-}Bu_3P)$ in the same solvent. The same spectral change was observed in the equimolar reaction of $MoO(dtb)_2$ with $n\text{-}Bu_3P$ in CH_2ClCH_2Cl. The transiently appeared absorption at 517 nm may be due to a reaction intermediate, which was successfully frozen at low temperatures; when $MoO(dtb)_2$ and $n\text{-}Bu_3P$ were dissolved in CH_2ClCH_2Cl below −40 °C, the solution spectrum with absorption maxima at 517 and 330 nm remained unchanged for several days at this temperature.

The presence of a reaction intermediate is confirmed also from ^{1}H NMR spectra of the $MoO(dtt)_2$–$n\text{-}Bu_3P$ system. Immediately after equimolar amounts of $MoO(dtt)_2$ and n-

---

[10] Newton, W. E.; Bravard, D. C.; McDonald, J. W. *Inorg. Nucl. Chem. Lett.* **1975**, *11*, 219.

Table I. ^{13}C NMR Chemical Shifts (ppm) and the ^{13}C-^{31}P Spin-Spin Coupling Constants (in Parentheses, Hz) of $MoO(dtb)_2$, $MoO(dtb)_2(n\text{-}Bu_3P)$, and the Reaction Intermediate in $CDCl_3$ (^1H Decoupled Spectra)

	C^{α}	$C^{\alpha'}$	C^1	$C^{1'}$	C^2	C^3	C^4
$MoO(dtb)_2$[a]	123.2		142.7		127.2	128.5	134.4
$MoO(dtb)_2(n\text{-}Bu_3P)$[a]	128.7 (6.4)	117.7	140.3 (3.7)	144.5	126.3, 126.6	127.3, 127.9	128.1, 128.9
reacn intermed[b]	not assigned	115.9 (14.0)	139.4 (<1)	143.5 (2.9)	not assigned		

[a] At room temperature. [b] At −45 °C.

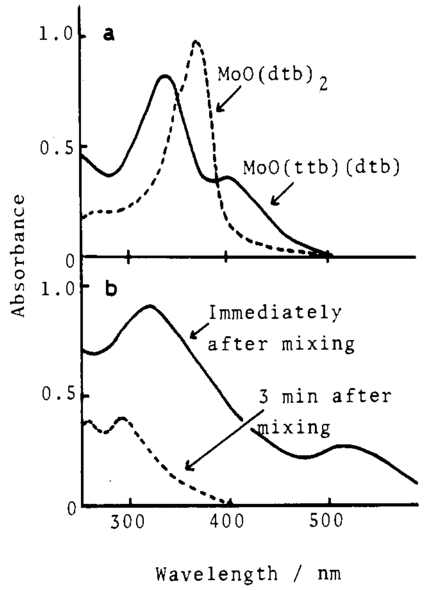

Figure 3. Electronic spectra of $MoO(ttb)(dtb)$ and $MoO(dtb)_2$ in CH_2ClCH_2Cl (a); the concentrations are both 5.0×10^{-4} mol dm^{-3}, and electronic spectra immediately after and 3 min after mixing $MoO(ttb)(dtb)$ (5.0×10^{-4} mol dm^{-3}) with 2 equiv of n-Bu_3P in CH_2ClCH_2Cl (b).

Bu_3P are mixed at −45 °C in $CDCl_3$, the solution exhibits two singlets due to the methyl protons (δ 2.40 and 2.43) and two quartets due to the phenyl ring protons (δ 8.03, 7.14 (J = 8 Hz) and δ 7.92, 7.02 (J = 8 Hz)), those having the same intensities (Figure 1c). All these signals are weakened with the rise of temperature, and alternatively a singlet signal (δ 2.31) and two quartet signals (δ 7.71, 7.08 (J = 8 Hz) and δ 7.59, 6.91 (J = 8 Hz)) newly appeared at −20 °C (Figure 1d). The final spectrum at room temperature was the same as the ^1H NMR spectrum of authentic $MoO(dtt)_2(n\text{-}Bu_3P)$ in $CDCl_3$. The lowest temperature spectrum (Figure 1c) may thus be assigned to the reaction intermediate formed between $MoO(dtt)_2$ and n-Bu_3P. The fact that there exist not only two AB patterns but also two methyl protons in magnetically different environments may exclude the trans configuration of the intermediate, in which n-Bu_3P coordinates to molybdenum from the bottom of the square-pyramidal structure of $MoO(dtt)_2$.

Figure 4 illustrates the ^1H decoupled and -coupled ^{13}C NMR spectra of $MoO(dtb)_2$ and $MoO(dtb)_2(n\text{-}Bu_3P)$ in $CDCl_3$ at room temperature together with the ^1H-decoupled spectrum immediately after $MoO(dtb)_2$ is mixed with an equimolar amount of n-Bu_3P in $CDCl_3$ at −45 °C.[11] The ^1H-decoupled ^{13}C NMR spectrum of $MoO(dtb)_2$ exhibits five resonances between 123.0 and 143.0 ppm downfield from Me_4Si (Figure 4a). These signals can tentatively be assigned by the first-order analysis of the ^1H-coupled ^{13}C NMR spectrum, as shown in Figure 4a and Table I. The ^1H-decoupled ^{13}C NMR spectrum of $MoO(dtb)_2(n\text{-}Bu_3P)$ displays eight resonances between 125.0 and 129.0 ppm downfield from Me_4Si (Figure 4b). Of these, a weak doublet signal centered at 128.7 ppm may be assigned to the C^{α} carbon coupled with ^{31}P (J = 6.4 Hz) because it remains unchanged in the ^1H-coupled ^{13}C NMR spectrum. The remaining six resonances are due to phenyl carbons except for C^1 and $C^{1'}$. The resonance at 117.7 ppm may be assigned to the $C^{\alpha'}$ carbon after comparing with the chemical shift of the C^{α} carbon of $MoO(dtb)_2$ (Figure 4a). No spin–spin coupling, however, is observed between the $C^{\alpha'}$ and ^{31}P nuclei, in contrast to the C^{α} nucleus. This is consistent with the cis configuration (**2**) of $MoO(dtt)_2$ (n-Bu_3P) described above, in which the $C^{\alpha'}$ atom is placed perpendicular to the equatorial plane involving the n-Bu_3P ligand. Similarly, the signal at 144.5 ppm assignable to $C^{1'}$ appears as a singlet, while the C^1 signal appears as a doublet at 140.3 ppm (J = 3.7 Hz) owing to spin–spin coupling with the ^{31}P nucleus (Figure 4b). Although the ^1H-decoupled ^{13}C NMR spectrum at −45 °C is not well resolved in the phenyl carbon region between 123.0 and 129.0 ppm owing to limited solubilities at low temperatures (Figure 4c), the general appearance is similar to that of the ^1H-decoupled spectrum of *cis*-$MoO(dtb)_2(n\text{-}Bu_3P)$ at room temperature (Figure 4b). It should, however, be noted that both the highest and the lowest ^{13}C signals in the spectrum at −45 °C (Figure 4c) occur as clear doublets owing to ^{13}C–^{31}P spin–spin couplings with J = 14 ($C^{\alpha'}$) and 2.9 Hz ($C^{1'}$), respectively, in contrast to the spectrum of $MoO(dtb)_2(n\text{-}Bu_3P)$ in which the corresponding signals appear as singlets. The spectrum at −45 °C may, therefore, be assigned to the reaction intermediate between $MoO(dtb)_2$ and n-Bu_3P. In order to acquire the structure of the intermediate, we measured the ^{13}C NMR spectrum of an equimolar mixture of CS_2 and n-Bu_3P in $CDCl_3$, which showed a doublet signal of the CS_2 carbon owing to spin–spin couplings with the ^{31}P nucleus (J(C–P) = 42 Hz). This rather large J value suggests the formation of the n-$Bu_3P{\cdot}CS_2$ adduct which may involve the C–P bond in solution. In fact, the $Et_3P{\cdot}CS_2$ adduct was isolated and the X-ray structure analysis has revealed the presence of a direct C–P bond with an atomic distance of 1.78 Å.[12] In view of these results, a possible structure for the reaction intermediate contains C–P interaction between $MoO(dtb)_2$ and n-Bu_3P, as shown in **3a**. The

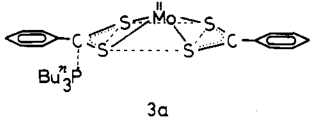

3a

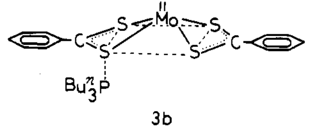

3b

$J(^{13}C^{\alpha'}$–$^{31}P)$ value of the intermediate (14 Hz), however, is considerably smaller than that of n-$Bu_3P{\cdot}CS_2$ (42 Hz). Thus, there may be another possible structure for the intermediate which involves a S–P bond as shown in **3b**. The structure **3b** may be supported from the ease with which sulfur abstracted from $MoO(ttb)(dtb)$ with n-Bu_3P, giving $MoO(dtb)_2$ and n-Bu_3PS.

Kinetics of the Reaction of $MoO(ttb)(dtb)$ with n-Bu_3P. The reaction of $MoO(ttb)(dtb)$ with n-Bu_3P was followed by monitoring the absorbances at 410 (λ_{max} = 404) and 517 nm,

---

[11] The ^1H-coupled ^{13}C NMR spectrum immediately after mixing $MoO(dtb)_2$ and n-Bu_3P in $CDCl_3$ at −45 °C has not been well obtained owing to low solubilities at this temperature.

[12] Margulis, T. N.; Templeton, D. H. *J. Am. Chem. Soc.* **1961**, *83*, 995.

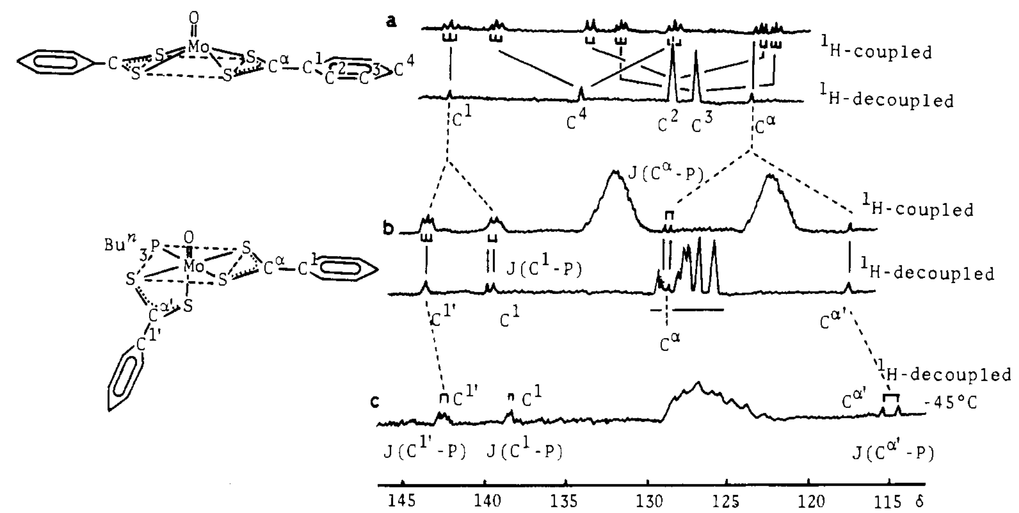

Figure 4. ^{13}C NMR spectra of MoO(dtb)$_2$ (a) and MoO(dtb)$_2$ (n-Bu$_3$P) (b) in CDCl$_3$ at room temperature and immediately after mixing MoO(dtb)$_2$ with n-Bu$_3$P in CDCl$_3$ at -45 °C (c).

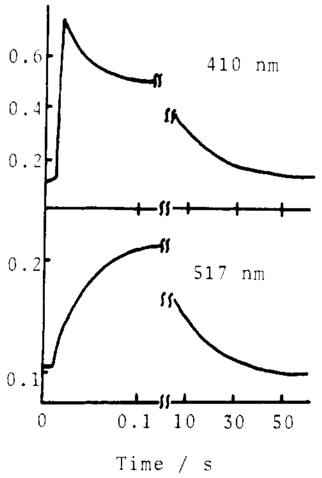

Figure 5. Changes of the absorbance with time for the reaction of MoO(ttb)(dtb) (5.0 × 10^{-5} mol dm^{-3}) with excess n-Bu$_3$P (1.0 × 10^{-3} mol dm^{-3}) in CH$_2$ClCH$_2$Cl at 25 °C.

which are due to MoO(ttb)(dtb) and the reaction intermediate, respectively. The decay or the rise of the absorbances at 410 and 517 nm are depicted in Figure 5, which shows that the reaction consists of two successive processes with half-lives of about 20 ms and 10 s. The reaction rates of these processes are different from each other sufficiently enough to allow the graphical determination of the rate constants. Plots of ln ($A_t - A_\infty$) vs. time for each process were found to be linear over a period 3 half-lives of the reaction. Pseudo-first-order rate constants, $k_{\rm obsd}{}^{(1)}$ (first step) and $k_{\rm obsd}{}^{(2)}$ (second step), were obtained by the least-squares method; each of the rate constants calculated from the change of the absorbance at 410 nm agreed with that at 517 nm. All the plots of $k_{\rm obsd}{}^{(1)}$ vs. the n-Bu$_3$P concentration at each temperature yield straight lines with a zero intercept, while $k_{\rm obsd}{}^{(2)}$ is essentially independent of the n-Bu$_3$P concentration at a given temperature, as shown in Figure 6a,b

The reaction of MoO(dtb)$_2$ with n-Bu$_3$P was followed by the change of the absorbances at 370 and 517 nm due to MoO(dtb)$_2$ and the intermediate, respectively. Both the absorbances immediately after the reactants were mixed in CH$_2$ClCH$_2$Cl exhibited only decay curves. This is because the formation process of the intermediate was too fast to detect it by the stopped-flow apparatus with a dead time of 0.5 ms. The rate constants obtained from the decay of the absorbances at 370 and 517 nm were independent of the n-Bu$_3$P concentration and in a good agreement with that of $k_{\rm obsd}{}^{(2)}$ in the

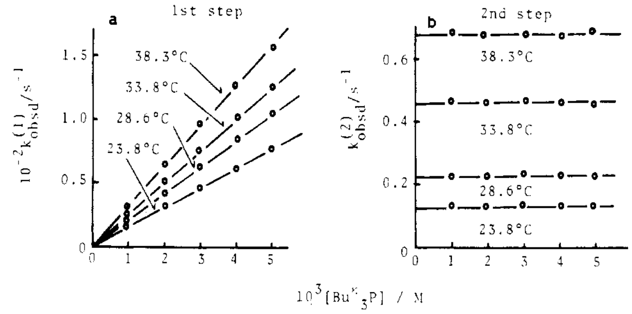

Figure 6. Plots of $k_{\rm obsd}{}^{(1)}$ (a) and $k_{\rm obsd}{}^{(2)}$ (b) vs. [n-Bu$_3$P] for the reaction of MoO(ttb)(dtb) (5.0 × 10^{-5} mol dm^{-3}) with n-Bu$_3$P in CH$_2$ClCH$_2$Cl.

Table II. Rate Constants and Activation Parameters for the Reaction of MoO(ttb)(dtb) with n-Bu$_3$P in CH$_2$ClCH$_2$Cl[a]

temp/°C	$10^{-4}k_1$/M^{-1} s^{-1}	$10k_2$/s^{-1}
23.8	2.85 ± 0.01	1.22 ± 0.04
28.6	3.31 ± 0.06	2.15 ± 0.05
33.8	3.55 ± 0.14	4.48 ± 0.18
38.3	3.84 ± 0.12	6.80 ± 0.02
$\Delta H^\ddagger_{298}$/kJ mol^{-1}	13 ± 3.1	90 ± 21.0
$\Delta S^\ddagger_{298}$/J mol^{-1} K^{-1}	-120 ± 1.7	42 ± 11.3

[a] Errors quoted are standard deviations.

reaction of MoO(ttb)(dtb) with n-Bu$_3$P. The present reaction can, therefore, be expressed as

$$\text{MoO(ttb)(dtb)} + n\text{-Bu}_3\text{P} \xrightarrow{k_1} \text{MoO(dtb)}_2 + n\text{-Bu}_3\text{PS} \quad (1)$$

$$\text{MoO(dtb)}_2 + n\text{-Bu}_3\text{P} \xrightarrow{\text{fast}} [\text{intermediate } \mathbf{3a} \text{ or } \mathbf{3b}] \quad (2)$$

$$[\text{intermeidate } \mathbf{3a} \text{ or } \mathbf{3b}] \xrightarrow{k_2} cis\text{-MoO(dtb)}_2(n\text{-Bu}_3\text{P}) \quad (3)$$

Equation 1 is the sulfur abstraction from MoO(ttb)(dtb) by n-Bu$_3$P, and eq 3 is the intramolecular rearrangment from the intermediate to *cis*-MoO(dtb)$_2$(n-Bu$_3$P). Table II lists the rate constants and activation parameters calculated from the Arrhenius plots of ln k vs. $1/T$. The activation entropy, $\Delta S_3{}^\ddagger$, for the sulfur abstraction reaction (eq 1) has a large negative value. In view of this result, the activated complex formed in the sulfur abstraction reaction may assume a structure in which n-Bu$_3$P is bound to the trithioperoxybenzoato CS$_3$ moiety of MoO(ttb)(dtb).

Kinetics of the Reaction of MoO(ttb)(dtb) with Ph$_3$P. Rates of the reaction of MoO(ttb)(dtb) with Ph$_3$P were measured from the decay of the absorbance at 410 nm. Pseudo-first-

Table III. Kinetic Parameters for the Reaction of MoO(ttb)(dtb) or $MoO(dtb)_2$ with Ph_3P in CH_2ClCH_2Cl

temp °C	$10^{-2}k_3/M^{-1}\ s^{-1}$	$10^{-3}k_4/s^{-1}$	k_{-4}/s^{-1}	K/M^{-1}
15.0	3.46 ± 0.29	0.67 ± 0.08	2.0	14.1 ± 1.3
20.0	4.30 ± 0.32	1.12 ± 0.14	4.0	10.1 ± 3.3
25.0	4.96 ± 0.08	2.15 ± 0.20	7.0	8.63 ± 3.0
30.0	5.50 ± 0.12	3.15 ± 0.26	13.0	4.71 ± 3.3
$\Delta H^{\ddagger}_{298}/kJ\ mol^{-1}$	19.0 ± 1.7	79.4 ± 6.4	92.1 ± 2.8	
$\Delta S^{\ddagger}_{298}/J\ mol^{-1}\ K^{-1}$	−130 ± 1.7	67.9 ± 21.6	63.9 ± 9.6	
$\Delta H^{\circ}_{298}/kJ\ mol^{-1}$				−43.6 ± 3.8
$\Delta S^{\circ}_{298}/J\ mol^{-1}\ K^{-1}$				−138 ± 13

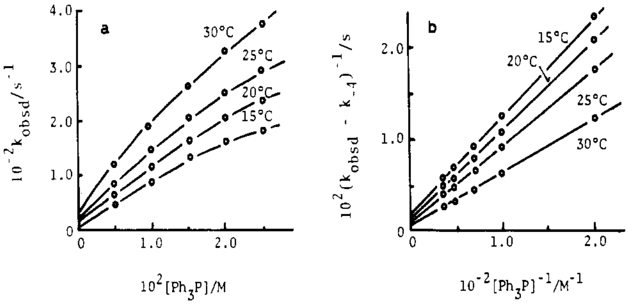

Figure 7. Plots of k_{obsd} vs. $[Ph_3P]$ (a) and $(k_{obsd} - k_{-4})^{-1}$ vs. $[Ph_3P]^{-1}$ (b) for the reaction of $MoO(dtb)_2$ (2.5×10^{-4} mol dm^{-3}) with excess Ph_3P in CH_2ClCH_2Cl.

order rate constants, k_{obsd}, were calculated from the slopes of the $\ln(A_t - A_\infty)$ vs. time plots at various concentrations of Ph_3P. Plots of the k_{obsd} value vs. the Ph_3P concentration at each temperature showed a straight line with a zero intercept, suggesting that the reaction is a nonequilibrium (eq 4). The

$$MoO(ttb)(dtb) + Ph_3P \xrightarrow{k_3} MoO(dtb)_2 + Ph_3PS \quad (4)$$

subsequent reaction between $MoO(dtb)_2$ and Ph_3P in excess, which is much faster than reaction 4, was followed independently by monitoring the decay of the absorbance at 370 nm which is due to $MoO(dtb)_2$. Plots of the k_{obsd} values obtained vs. the Ph_3P concentration give a gentle grade with nonzero intercepts, as shown in Figure 7a. This indicates that the reaction is an equilibrium one which may involve *trans*- and *cis*-$MoO(dtb)_2(Ph_3P)$ and the dissociative species in solution (eq 5 and 6), as described in the previous section. The

$$MoO(dtb)_2 + Ph_3P \overset{K}{\rightleftharpoons} trans\text{-}MoO(dtb)_2(Ph_3P) \quad (5)$$

$$trans\text{-}MoO(dtb)_2(Ph_3P) \underset{k_{-4}}{\overset{k_4}{\rightleftharpoons}} cis\text{-}MoO(dtb)_2(Ph_3P) \quad (6)$$

formation of the trans adduct (eq 5) is reasonably suggested from the assumption that Ph_3P would coordinate at a vacant site trans to the oxo ligand of $MoO(dtb)_2$ with a square-pyramidal configuration. It should, however, be mentioned that there has been no spectroscopic evidence for the formation of a precursor complex similar to **3a** or **3b** prior to the formation of the trans adduct. This is compatible with no appreciable interaction of Ph_3P with CS_2, as confirmed from electronic (in CH_2ClCH_2Cl) and ^{13}C NMR (in $CDCl_3$) spectra, in contrast to the C–P bond formation between CS_2 and $n\text{-}Bu_3P$ as described above. Thus, the mechanistic difference between the reactions of Ph_3P and $n\text{-}Bu_3P$ toward $MoO(dtb)_2$ may be due to a weaker donor property of Ph_3P than $n\text{-}Bu_3P$. If one can assume that the adduct formation (eq 5) is much faster than the trans–cis isomerization (eq 6), the observed rate constant, k_{obsd}', for the reaction of $MoO(dtb)_2$ with excess Ph_3P is expressed as eq 7. This equation can be transformed to

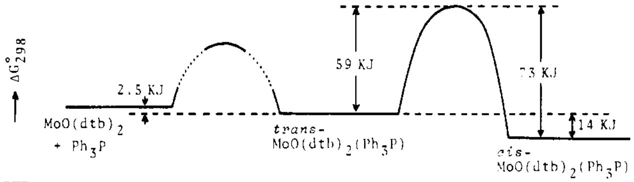

Figure 8. Reaction coordinates for the reaction of $MoO(dtb)_2$ with Ph_3P.

$$k_{obsd}' = \frac{(k_4 + k_{-4})K[Ph_3P] + k_{-4}}{1 + K[Ph_3P]} \quad (7)$$

$$\frac{1}{k_{obsd}' - k_{-4}} = \frac{1}{k_4} + \frac{1}{k_4K[Ph_3P]} \quad (8)$$

eq 8, which shows a linear relation between $1/(k_{obsd}' - k_{-4})$ vs. $1/[Ph_3P]$, although the correct value of k_{-4} cannot be determined from Figure 7a. Thus, the k_{-4} value has been determined in such a way that plots of $1/(k_{obsd}' - k_{-4})$ vs. $1/[Ph_3P]$ give straight lines (correlation coefficient >0.999) at several temperatures, as depicted in Figure 7b. Moreover, the rate constant k_2 and the equilibrium constant K were determined from the intercept and the slopes of the straight lines of Figure 7b. The rate and equilibrium constants thus obtained are listed in Table III, which shows also the thermodynamic and activation parameters obtained from the Arrhenius plots. The k_3 value is about 30 times smaller than that of $(k_4 + k_{-4})K$ of eq 7. Thus, the rate-determining step for the reaction of MoO(ttb)(dtb) with excess Ph_3P is the sulfur abstraction (eq 4), and the k_{obsd} for eq 4 can be expressed as eq 9. The ratio of the rate constants, k_4/k_{-4}, for the

$$k_{obsd} = k_1[Ph_3P] \quad (9)$$

trans–cis isomerization process (eq 6) are in the range of about 150–250, suggesting that the trans isomer is less stable than the cis isomer. The reaction of $MoO(dtb)_2$ with Ph_3P can, therefore, be illustrated by the reaction coordinate shown in Figure 8. On the other hand, both the activation entropies for the trans–cis isomerization, $\Delta S_4^{\ddagger}$ and $\Delta S_{-4}^{\ddagger}$, are positive values with the same order of magnitude. This result leads us to the conclusion that the transition state in the trans–cis isomerization would involve the ring opening of a chelate dtb ligand.

Registry No. MoO(ttb)(dtb), 71900-01-1; $n\text{-}Bu_3P$, 998-40-3; Ph_3P, 603-35-0; $MoO(dtb)_2(n\text{-}Bu_3P)$, 81230-35-5; *cis*-$MoO(dtb)_2(Ph_3P)$, 81230-36-6; *trans*-$MoO(dtb)_2(Ph_3P)$, 81275-48-1; $MoO(dtb)_2$, 81230-37-7; MoO(ttt)(dtt), 81230-38-8; $MoO(dtt)_2(n\text{-}Bu_3P)$, 81230-39-9; $MoO(dtt)_2$, 81230-40-2.